Review Article

Cardiac computed tomography radiomics: a narrative review of current status and future directions

Jin Shang[1], Yan Guo[2], Yue Ma[1], Yang Hou[1]

[1]Department of Radiology, Shengjing Hospital of China Medical University, Shenyang, China; [2]GE Healthcare, Beijing, China

Contributions: (I) Conception and design: Y Hou, J Shang; (II) Administrative support: Y Hou; (III) Provision of study materials or patients: Y Guo, Y Ma; (IV) Collection and assembly of data: J Shang, Y Guo; (V) Data analysis and interpretation: J Shang; (VI) Manuscript writing: All authors; (VII) Final approval of manuscript: All authors.

Correspondence to: Yang Hou. Department of Radiology, Shengjing Hospital of China Medical University, 36 Sanhao Street, Heping District, Shenyang 110004, China. Email: houyang1973@163.com.

Background and Objective: In an era of profound growth of medical data and rapid development of advanced imaging modalities, precision medicine increasingly requires further expansion of what can be interpreted from medical images. However, the current interpretation of cardiac computed tomography (CT) images mainly depends on subjective and qualitative analysis. Radiomics uses advanced image analysis to extract numerous quantitative features from digital images that are unrecognizable to the naked eye. Visualization of these features can reveal underlying connections between image phenotyping and biological characteristics and support clinical outcomes. Although research into radiomics on cardiovascular disease began only recently, several studies have indicated its potential clinical value in assessing future cardiac risk and guiding prevention and management strategies. Our review aimed to summarize the current applications of cardiac CT radiomics in the cardiovascular field and discuss its advantages, challenges, and future directions.

Methods: We searched for English-language articles published between January 2010 and August 2021 in the databases of PubMed, Embase, and Google Scholar. The keywords used in the search included computed tomography or CT, radiomics, cardiovascular or cardiac.

Key Content and Findings: The current applications of radiomics in cardiac CT were found to mainly involve research into coronary plaques, perivascular adipose tissue (PVAT), myocardial tissue, and intracardiac lesions. Related findings on cardiac CT radiomics suggested the technique can assist the identification of vulnerable plaques or patients, improve cardiac risk prediction and stratification, discriminate myocardial pathology and etiologies behind intracardiac lesions, and offer new perspective and development prospects to personalized cardiovascular medicine.

Conclusions: Cardiac CT radiomics can gather additional disease-related information at a microstructural level and establish a link between imaging phenotyping and tissue pathology or biology alone. Therefore, cardiac CT radiomics has significant clinical implications, including a contribution to clinical decision-making. Along with advancements in cardiac CT imaging, cardiac CT radiomics is expected to provide more precise phenotyping of cardiovascular disease for patients and doctors, which can improve diagnostic, prognostic, and therapeutic decision making in the future.

Keywords: Cardiac computed tomography; radiomics; phenotyping; cardiovascular disease

Submitted Oct 16, 2021. Accepted for publication Mar 23, 2022.
doi: 10.21037/qims-21-1022
View this article at: https://dx.doi.org/10.21037/qims-21-1022

Introduction

As a non-invasive imaging tool, cardiac computed tomography (CT) has experienced a dramatic evolution from identifying anatomically significant coronary artery stenosis to become an advanced imaging tool that plays an increasingly important role in guiding clinical decision-making in various fields of cardiovascular medicine (1-6). In particular, the development of coronary computed tomography angiography (CCTA) has advanced the assessment of suspected coronary artery disease (CAD) (7). Although advances in CT techniques have enabled radiological examinations to provide a wide variety of information, the current data-analysis and image interpretation techniques still mostly rely on qualitative evaluation determined by radiological experts (8). The rise of precision medicine requires us to provide more quantitative information in order to detect subtle changes related to underlying pathologic processes and improve the diagnostic acuity of imaging examinations, while reducing subjectivity and bias (9).

Radiomics is contrary to the traditional practice of regarding medical images as pictures that can only be used for visual interpretation. Radiomics refers to the process of extracting vast amounts of data regarding the quantitative features of a given region of interest (ROI) to create large datasets that can be subsequently mined to reveal the relationships between distinct radiomics metrics to improve clinical decision making (8). So far, radiomics has been successfully applied to oncology research. Previous research has shown that radiomics can help with the precise diagnosis of tumors (10), prediction of clinical outcomes (11,12), monitoring of disease progression (13), and assessment of therapeutic response and prognosis (13-15). Since the development of the radiomics quality score and image biomarker standardization initiative, radiomics has become increasingly standardized (16,17).

Radiomics could provide a bridge between cardiac CT images and cardiovascular medicine. Although radiomics research based on cardiac CT began relatively recently, several proof-of-concept studies have found its incremental value in the cardiovascular field (18-25). The purpose of this review was to summarize the current applications of cardiac CT radiomics in the cardiovascular field and discuss its advantages, challenges, and future directions. We present the following article in accordance with the Narrative Review reporting checklist (available at https://qims.amegroups.com/article/view/10.21037/qims-21-1022/rc).

Methods

We searched the databases of PubMed, Embase, and Google Scholar for articles that had been published between January 2010 and August 2021. A combination of keywords, computed tomography or CT, radiomics, cardiovascular or cardiac, were used. Two investigators with an experience of 5 years in cardiovascular imaging diagnosis independently checked each identified article for inclusion criteria. Disagreements were discussed and resolved by consensus (*Table 1*). The inclusion criteria were as follows: (I) the articles reported the value of radiomics based on cardiac CT in the cardiovascular disease; (II) the articles were published in English. The exclusion criteria were as follows: (I) reviews, letters, editorials, comments, case reports and unpublished articles were excluded. Finally, a total of 17 articles were selected. Then, the full articles were read carefully and the relevant information on the application value of cardiac CT radiomics were extracted.

Radiomics characterization

Radiomics is the process of extracting vast amounts of data of quantitative features from tomographic images for the purpose of converting digital images to higher-dimensional mineable data that can subsequently be used to improve clinical decision support (26). A common workflow of radiomics is composed of image acquisition and preprocessing, image segmentation, feature extraction and selection, model building and validation (16) (*Figure 1*). Radiomics data mainly contain first-order, second-order, and higher-order statistics that represent a massive number of features linked with the shape, attenuation, volume, and texture of a given lesion (26). The tomographic images collected with radiomics are more than pictures—they are data (16,26). These data are calculated by complicated mathematical formulae and may recognize features that are undiscernible to the naked eye. Given its characteristics, radiomics may establish an undiscovered correlation between imaging features and significant clinical outcomes.

Current applications of cardiac CT radiomics

The current applications of radiomics for cardiac CT mainly involve research surrounding coronary plaques, perivascular adipose tissue (PVAT), myocardial tissue, and intracardiac lesions (*Figure 2*). A comprehensive

Table 1 Summary of the literature search strategy

Items	Specification
Date of search (specified to date, month, and year)	10 August, 2021
Databases and other sources searched	PubMed, Embase, and Google Scholar
Search terms used (including MeSH and free text search terms and filters)	Computed tomography or CT; radiomics; cardiovascular or cardiac
Timeframe	January 2010 to August 2021
Inclusion and exclusion criteria (study type, language restrictions etc.)	Inclusion criteria: (I) the articles reported the value of radiomics based on cardiac CT in the cardiovascular disease; (II) the articles were published in English. Exclusion criteria: (I) reviews, letters, editorials, comments, case reports and unpublished articles were excluded
Selection process (who conducted the selection, whether it was conducted independently, how consensus was obtained, etc.)	Study selection was conducted by two investigators. Disagreements were discussed and resolved by consensus
Any additional considerations, if applicable	

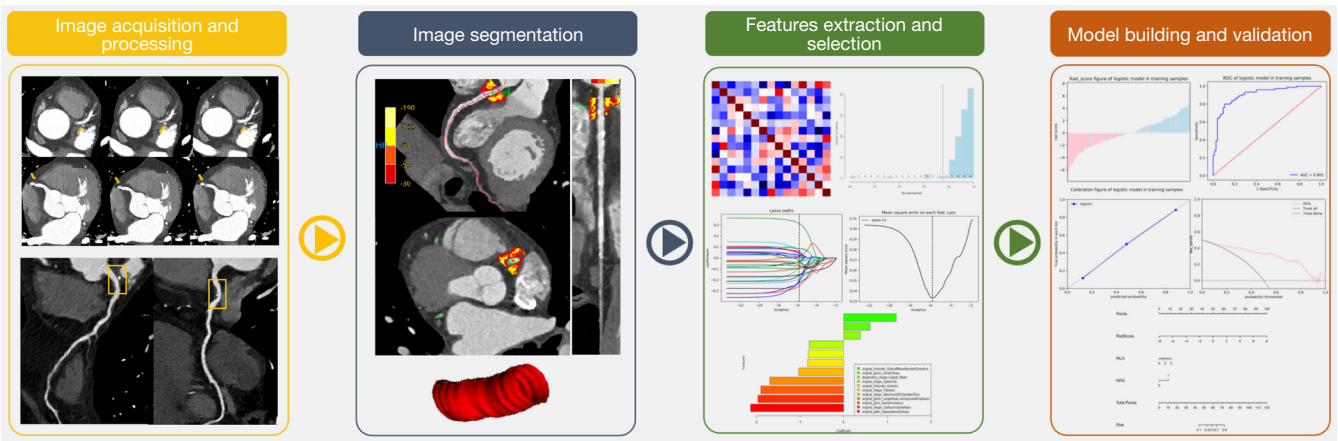

Figure 1 A common workflow of radiomics. Radiomics workflow is commonly composed of image acquisition and preprocessing, image segmentation, feature extraction and selection, model building and validation. The yellow arrow and frame refer to the coronary plaques in the axial and multiplanar reconstruction images based on CCTA, respectively.

overview of current applications of cardiac CT radiomics in cardiovascular disease is presented in *Table 2*.

Radiomics phenotyping of coronary plaques

As a first-line diagnostic tool to detect and characterize coronary atherosclerosis, CCTA is used to evaluate coronary luminal stenosis and visualize coronary atherosclerosis changes including plaque composition, distribution, and burden. Although increasing evidence suggests that the presence of high-risk plaque (HRP) confers an increased risk of major adverse cardiac events (MACE) and provides additional prognostic information, identification of HRP features still relies on expert experience and tends to vary between different observers or intra-observers (37-43). Furthermore, HRP characteristics derived from CCTA are only suitable to identify visible atherosclerosis at advanced stages, but it would be desirable to visualize the early pathophysiological process of atherosclerosis including inflammation, apoptosis, or cell migration (44). Radiomics might provide us with more objective parameters to overcome limitations of subjective visual assessment and describe the nature changes of a given plaque, such as texture and spatial complexity (8).

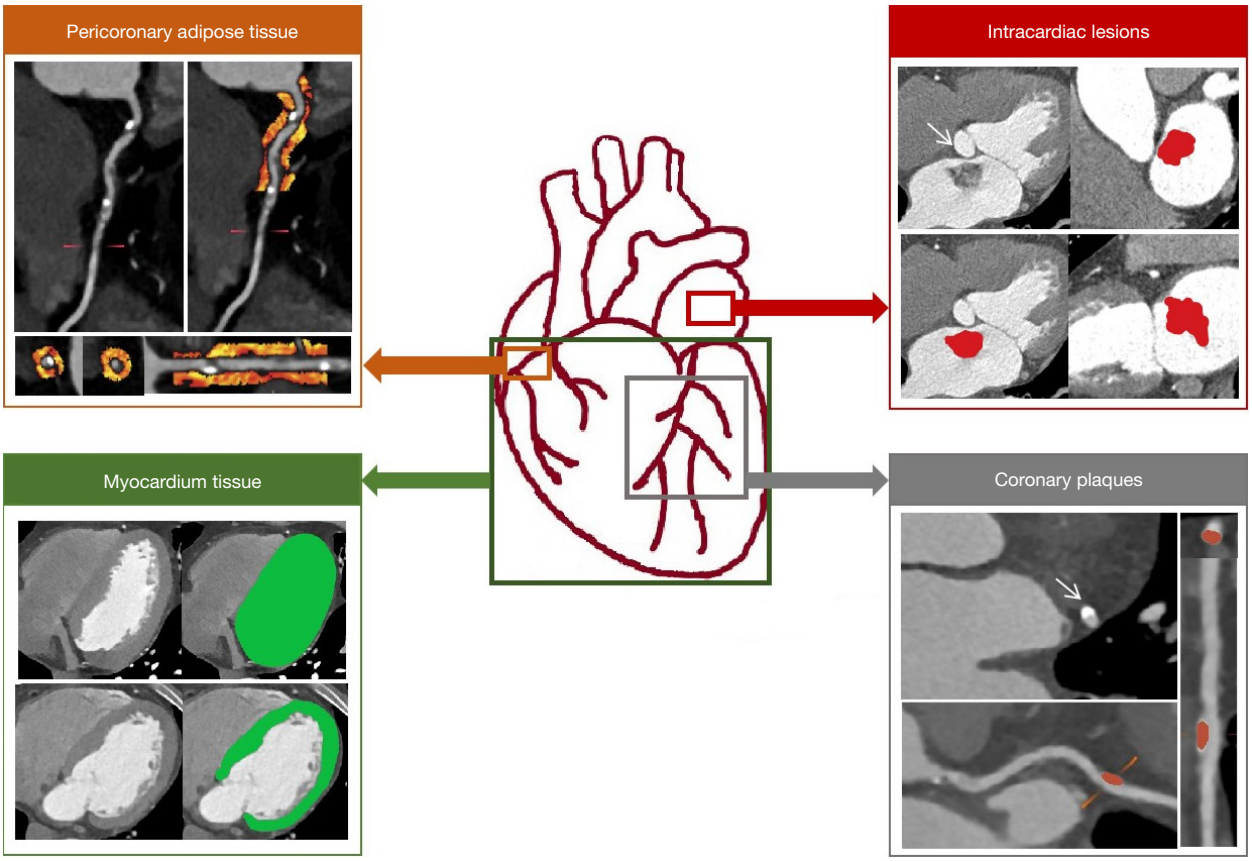

Figure 2 The current applications of cardiac CT radiomics. The current applications of radiomics on cardiac CT mainly focus on coronary plaques, pericoronary adipose tissue, myocardial tissue, and intracardiac lesions. CT, computed tomography. The white arrow above refers to the lesion of left atrium. The white arrow below refers to the coronary plaque.

Identification of plaque vulnerability

In an initial study exploring the potential of radiomics in atherosclerosis plaques, Kolossváry *et al.* (18) used the radiomics approach to extract 4,440 radiomic parameters from coronary plaques with and without the napkin-ring sign (NRS) (*Figure 3*). They compared them with 8 conventional quantitative parameters and found that more than 20% of radiomic features were significantly different between plaques with or without NRS. This suggested that radiomics features can potentially identify a qualitative NRS feature. Another study by Kolossváry *et al.* (20) demonstrated that a radiomics-based machine learning model of CCTA displayed superior diagnostic performance [area under the curve (AUC) =0.73] in the identification of advanced atherosclerotic plaques compared with that of visual assessment (AUC =0.65; P=0.04) and compared with histogram-based measurements of areas with low CT attenuation (AUC =0.55; P=0.01) and an average Hounsfield unit (HU; AUC =0.53; P=0.004). Additionally, an analysis of 44 plaques from 25 patients with suspected CAD who underwent multiple imaging examinations showed that CCTA-based radiomic analyses had superior diagnostic accuracy than conventional plaque features to identify invasive and radionuclide imaging markers of plaque vulnerability (21).

Identification of significant myocardial ischemia

To explore the superiority of CCTA-based coronary plaque radiomics in the identification of myocardial ischemia, Hu *et al.* (19) extracted 1,409 radiomics features from 105 coronary plaques of 88 patients who underwent CCTA and invasive fractional flow reserve (FFR), simultaneously compared them with conventional CCTA features. They found that 3 quantitative wavelet features were closely related to myocardial ischemia, and the CCTA-based radiomics model (AUC =0.762) outperformed the

Table 2 A comprehensive overview of current applications on cardiac CT radiomics in cardiovascular disease

Study	ROI segmentation	Application	Study design	Patient characteristics	Main performance
Kolossváry *et al.* (18) (2017)	Coronary plaques	Napkin-ring sign (NRS)	30 patients with NRS plaques *vs.* 30 non-NRS plaques	30 patients caused by stable chest pain [NRS group: mean age of 63.07 (56.54, 68.36) years, 20% female; non-NRS group: mean age of 63.96 (54.73, 72.13) years, 33% female]	Radiomics parameters: short- and long-run low gray-level emphasis and surface ratio of high attenuation voxels to total surface had the highest area under the curve values (AUC: 0.918, 0.894 and 0.890, respectively)
Kolossváry *et al.* (20) (2019)	Coronary plaques	Advanced atherosclerotic lesions	445 cross sections including early atherosclerotic lesions (n=311) and advanced atherosclerotic lesions (n=134) of 21 coronary arteries from seven hearts	Seven hearts obtained from male donors (mean age of 52.3±5.3 years)	Radiomics-based ML model (AUC: 0.73, 95% CI: 0.63–0.84) Visual assessment (AUC: 0.65, 95% CI: 0.56–0.73) Area of low attenuation (AUC: 0.55, 95% CI: 0.42–0.68) Average Hounsfield unit (AUC: 0.53, 95% CI: 0.42–0.65)
Kolossváry *et al.* (21) (2019)	Coronary plaques	Attenuated plaque by IVUS; Thin-cap fibroatheroma by OCT; NaF^{18} -positivity	44 plaques of 25 patients who underwent CCTA, $Na^{18}F$-PET, IVUS, and OCT.	25 patients with suspected CAD (mean age of 62[59, 69] years, 23 males)	Attenuated plaque by IVUS (fractal box counting dimension of high attenuation voxels *vs.* non-calcified plaque volume, AUC: 0.72, 95% CI: 0.65–0.78 *vs.* 0.59, 95% CI: 0.57–0.62) Thin-cap fibroatheroma by OCT (fractal box counting dimension of high attenuation voxels *vs.* presence of low attenuation voxels, AUC: 0.80, 95% CI: 0.72–0.88 *vs.* 0.66, 95% CI: 0.58–0.73) $Na^{18}F$-positivity (surface of high attenuation voxels *vs.* presence of two high-risk features, AUC: 0.87, 95% CI: 0.82–0.91 *vs.* 0.65, 95% CI: 0.64–0.66)
Hu *et al.* (19) (2020)	Coronary plaques	Myocardial ischaemia	105 coronary plaques of 88 patients who underwent CCTA and invasive FFR	88 patients (FFR ≤0.8 group (n=38): mean age of 62.5±8.3 years, 24 males; FFR >0.8 group (n=50): mean age of 61.2±8.2 years, 36 males)	Radiomics model significantly outperformed conventional model in identifying myocardial ischemia in the training (AUC: 0.762, 95% CI: 0.671–0.853 *vs.* 0.631, 95% CI: 0.519–0.742) and validation set (AUC: 0.671, 95% CI: 0.466–0.875 *vs.* 0.592, 95% CI: 0.519–0.742)
Li *et al.* (27) (2021)	Coronary plaques	Ischemic coronary stenosis	174 plaques of 149 patients with at least one lesion stenosis degree between 30% and 90%	149 patients (mean age of 62.21±8.47 years, 96 males) with suspected or known stable CAD	CCTA-based radiomic model were superior to conventional plaques model in identifying hemodynamically significant coronary stenosis in the training (AUC: 0.82, 95% CI: 0.73–0.90 *vs.* 0.71, 95% CI: 0.61–0.80) and validation set (AUC: 0.77, 95% CI: 0.60–0.93 *vs.* 0.70, 95% CI: 0.52–0.88) respectively

Table 2 *(continued)*

Table 2 *(continued)*

Study	ROI segmentation	Application	Study design	Patient characteristics	Main performance
Oikonomou *et al.* (23) (2019)	PVAT of proximal RCA and LCA	Study 1: Adipose tissue inflammation (TNFA expression), adipose tissue fibrosis (COL1A1 expression), adipose tissue vascularity (CD31 expression)	Study 1: 167 adipose tissue biopsies from cardiac surgery patients undergoing CCTA	Study 1: 167 adipose tissue biopsies from cardiac surgery patients {mean age of 67 [59, 74] years; 27 females}	Study 1: Wavelet-transformed mean attenuation is associated with adipose tissue inflammation (TNFA expression), radiomic texture features are connected with adipose tissue fibrosis (COL1A1 expression) and vascularity (CD31 expression)
		Study 2: MACE (cardiac mortality and non-fatal acute myocardial infarction and revascularization events)	Study 2: 101 patients experienced MACE within 5 years of a CCTA scan *vs.* 101 matched controls who had no cardiac event during the same follow-up period	Study 2: 101 patients with MACE {mean age of 64 [55, 72] years; 34 females} *vs.*101 patients without MACE {mean age of 62 [53, 70] years; 34 females}	Study 2: FRP signature significantly improved MACE prediction beyond traditional risk stratification [Δ(C-statistic) =0.126, P<0.001]
		Study 3: AMI *vs.* stable CAD	Study 3: 44 AMI patients *vs.* 44 stable CAD controls	Study 3: 44 AMI patients {mean age of 62 [53, 72] years; 37 males} *vs.* 44 stable CAD {mean age of 62 [51, 70] years; 28 males}	Study 3: FRP is significantly higher in patients with AMI than stable CAD controls (P<0.001). In a subgroup analysis of 16 AMI patients who underwent sequential CCTA scanning, there were no significant changes of FRP values within 96 hours of admission for AMI and 6 months later, but perivascular FAI around the RCA changed at 6 months
Lin *et al.* (24) (2020)	PCAT around proximal RCA; PCAT around culprit and nonculprit lesions	Acute MI *vs.* stable or no CAD	60 patients with acute MI *vs.* 60 patients with stable CAD *vs.* 60 controls with no CAD	60 patients with acute MI (mean age of 58.4 [51.6, 73.7] years, 52 males) *vs.* 60 patients with stable CAD {mean age of 60.0 [52.0, 68.5] years, 52 males) *vs.* 60 controls with no CAD (mean age of 59.5 [52.0, 69.0] years, 52 males}	Radiomics-based model (AUC: 0.87, 95% CI: 0.82–0.93) outperformed PCAT attenuation-based model (AUC: 0.77, 95% CI: 0.70–0.84) and clinical model (AUC: 0.76, 95% CI: 0.69–0.84) in identifying patients with acute MI At 6 months post-MI, there was no significant change in the PCAT radiomic profile around the proximal RCA or non-culprit lesions
Shang *et al.* (28) (2021)	PCAT around culprit lesions in ACS and the highest-grade stenosis nonculprit lesions in control group	Acute coronary syndrome (ACS)	90 patients with subsequent ACS within 3 years *vs.* 90 patients without adverse cardiac events.	Of the 180 patients with suspected CAD, training set (n=134): ACS group with 51 males (mean age of 62.88±10.81 years), control group with 46 males (mean age of 62.61±10.81 years); testing set (n=46): ACS group with 14 males (mean age of 65.43±7.42 years), control group with 17 males (mean age of 63.09±7.82 years)	Radiomics score achieved superior performance in identifying patients with future ACS within 3 years in both training and test datasets (AUC =0.826, 0.811) compared with plaque score (AUC =0.699, 0.640), while the improvement of integrated score discriminating capability (AUC =0.838, 0.826) was non-significant

Table 2 *(continued)*

Table 2 *(continued)*

Study	ROI segmentation	Application	Study design	Patient characteristics	Main performance
Mannil *et al.* (29) (2018)	Left ventricular myocardium and blood pool	Myocardial infarction (MI)	27 patients with acute MI *vs.* 30 patients with chronic MI *vs.* 30 controls without cardiac abnormality who underwent non-contrast-enhanced low radiation dose CCT	27 patients with acute MI (mean age of 60±12 years, 9 females) *vs.* 30 patients with chronic MI (mean age of 68±13 years, 8 females) *vs.*30 patients with chronic MI (mean age of 44±6 years, 9 females)	Model I: Controls *vs.* Acute MI *vs.* Chronic MI The best classification results were obtained using the k-nearest neighbors classifier (sensitivity: 69%, specificity: 85%, false-positive rate: 0.15) Model II: Controls *vs.* Acute and chronic MI The best classification results were obtained by the locally weighted learning classification (sensitivity: 86%, specificity: 81%, false-positive rate:0.19) with an AUC of 0.78
Hinzpeter *et al.* (22) (2017)	Left ventricular myocardium	Acute myocardial infarction (AMI)	20 patients with AMI *vs.* 20 controls with no cardiac abnormalities who underwent contrast-enhanced cardiac CT	20 patients with AMI (mean age of 56±10 years, 5 females) *vs.* 20 patients (mean age of 42±15 years, 8 females)	The best model combining kurtosis and SRHGE (AUC: 0.9, 95% CI: 0.80–0.99) had the best diagnostic performance in the prediction of acute MI The best results for kurtosis and SRHGE were obtained at a 5 mm slice thickness (AUC: 0.78)
Kay *et al.* (30) (2020)	Left ventricle	High-risk left ventricular hypertrophy	1,982 participants who underwent CAC-CT and CMR	1,587 patients of training subset (mean age of 51.09±9.56 years, 642 males); 395 patients of validation subset (mean age of 51.52±9.91 years, 172 males)	The diagnostic performance of cluster-based LR, LR without highly correlated features, optimal LASSO model and simplest LASSO modes for identifying high-risk left ventricular hypertrophy based on CAC-CT were 0.74 (95% CI: 0.67–0.82), 0.74 (95% CI: 0.67–0.81), 0.76 (95% CI: 0.69–0.83,) and 0.73 (95% CI: 0.66–0.80), respectively
Antunes *et al.* (31) (2016)	Left ventricular myocardium and blood pool	Scarred myocardium	7 patients with myocarditis who underwent delayed iodine enhanced CCT	7 patients with post-myocarditis scars and implantable cardioverter defibrillator	The diagnostic accuracy of specific energy feature derived from the baseline scan in the differentiation between normal and scarred myocardium was 94%
Esposito *et al.* (32) (2018)	Left ventricular remote myocardium	Myocardial heterogeneity	48 patients with recurrent ventricular tachycardia who underwent late iodine enhancement CCT	Of the 48 patients with recurrent ventricular tachycardia (mean age of 61±15 years, 44 males), 5 had IVT, 23 had ICM, 9 had IDCM, and 11 had MYO	Patients with ICM and IDCM had higher values of SD and MAD than patients with MYO and IVT, independently of LV volume systolic and diastolic function Myocardial heterogeneity (SD and MAD) was associated with LV dilatation, systolic and diastolic function
Shu *et al.* (33) (2020)	Left ventricular myocardium	Chronic myocardial ischemia	154 patients with CAD undergoing CCTA and SPECT-MPI	Of the 154 patients, training set (n=107): mean age of 60.5±14.9 years, 75 males; test set (n=47): mean age of 60.7±13.4 years, 29 males; verification (n=49): mean age of 64.1±11.5 years, 29 males	The diagnostic accuracy of the nomogram, signature, and vascular stenosis for the prediction of MIS were 0.824, 0.736 and 0.708, respectively The radiomics nomogram detected a significant difference in the number of patients with MIS between the high and low-risk groups (P<0.05)

Table 2 *(continued)*

Table 2 *(continued)*

Study	ROI segmentation	Application	Study design	Patient characteristics	Main performance
Nam *et al.* (34) (2019)	Periprosthetic Mass	Causes of PVO	39 periprosthetic masses of 34 patients who were clinically suspected as PVO and underwent CCT	39 periprosthetic masses (20 cases of pannus, 11 thrombi, and 8 vegetations) in 34 patients (mean age of 55.8±11.2 years, 14 males)	The AUC of radiomic score for differentiation of pannus from other causes of PVO was 0.876 (95% CI: 0.731–0.960) A combination of radiomic score and visual analysis showed better performance for the differentiation of pannus than visual analysis alone
Qian *et al.* (35) (2021)	Cardiac myxomas	Cardiac myxomas	59 CMs *vs.* 50 cardiac thrombi from 109 patients who underwent cardiovascular contrast-enhanced computed tomography	59 CMs (mean age of 61.6±12.6 years, 33 females) *vs.* 50 cardiac thrombi (mean age of 58.5±14.5, 23 females)	A radiomics signature performed better in differentiating cardiac myxomas from cardiac thrombi than the conventional clinical model (AUC: 0.926 and 0.878, respectively)
Chun *et al.* (36) (2020)	LAA filling defects	LAA thrombus	95 patients with valvular heart disease and filling defects in LAA who underwent early- and late-phase CCT	95 patients with valvular heart disease (mean age of 65.1±9.9 years, 44 males)	Wavelet_LHL and wavelet_LLH (AUC: 0.78, 95% CI: 0.69–0.86, both) had the highest diagnostic performance for differentiating LAA thrombus from circulatory stasis among the 8 selected radiomic features Compared with wavelet_LHL, LAA/AA_E showed significantly lower diagnostic performance (P=0.025), whereas LAA/AA_L and ΔLAA/AA were not significantly different (P=0.773 for LAA/AA_L and P=0.230 for ΔLAA/AA)

FRP refers to the product of a random forest model to discriminate MACE from non-MACE cases. PVAT refers to all the voxels between −190 and −30 HU range located within a radial distance from the outer vessel wall equal to the average diameter of the respective vessel. Values are mean ± SD or median [25th, 75th percentile]. ACS, acute coronary syndrome; AUC, area under the curve; CAC-CT, non-contrast cardiac computed tomography; CAD, coronary artery disease; CCT, cardiac computed tomography; CCTA, coronary computed tomography angiography; CD31, cluster of differentiation 31; CI, confidence interval; CM, cardiac myxoma; CMR, cardiac magnetic resonance; COL1A1, collagen type 1 alpha 1; CT, computed tomography; CTA, computed tomography angiography; ECV, extracellular volume; FFR, fractional flow reserve; FRP, fat radiomic profile; HRP, high-risk plaque; ICM, ischemic cardiomyopathy; IDCM, idiopathic dilated cardiomyopathy; IQR, interquartile range; IVT, idiopathic ventricular tachycardia; IVUS, intravascular ultrasound; LAA, left atrial appendage; LAA/AA, left atrial appendage/ascending aorta. LAD, left anterior descending; LASSO, least absolute shrinkage and selection operator; LCA, left coronary artery; LR, logistic regression; LV, left ventricle; MACE, major adverse cardiovascular events; MAD, mean absolute deviation; MI, myocardial infarction; MIS, chronic myocardial ischemia; ML, machine learning; MPI, myocardial perfusion imaging; MYO, post-myocarditis syndrome; NaF18-PET, sodium fluoride-18 positron emission tomography; NRS, napkin-ring sign; OCT, optical coherence tomography; PCAT, pericoronary adipose tissue; PVAT, perivascular adipose tissue; PVO, prosthetic valve obstruction; RCA, right coronary artery; ROI, region of interest; SD, standard deviation; SPECT, single photon emission computed tomography; SRHGE, short run high gray-level emphasis; TNFA, tumor necrosis factor alpha.

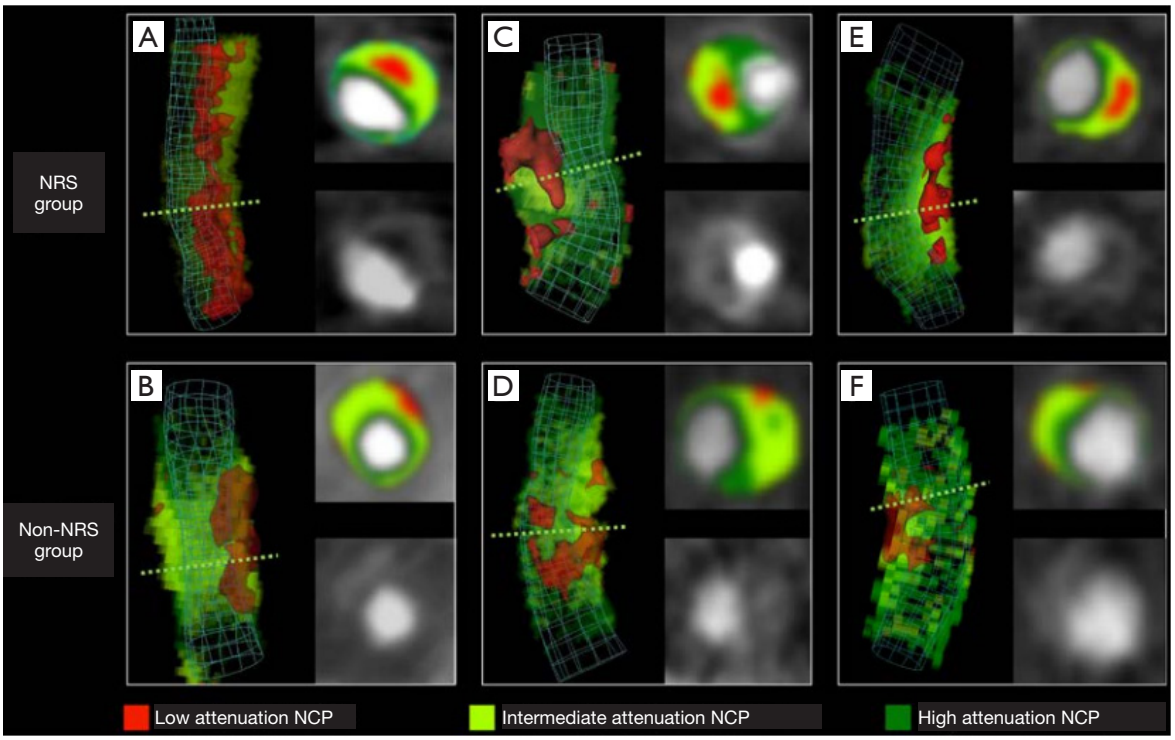

Figure 3 Representative examples of plaques with and without the NRS. Volume-rendered and cross-sectional images of plaques with NRS in the top (A, C, and E) and their matched plaques in the bottom (B, D, and E) are shown. Green dashed lines indicate the location of cross-sectional planes. Colors indicate different computed tomographic attenuation values [reproduced with permission from reference (18)]. NCP, non-calcified plaque; NRS, napkin-ring sign.

conventional model in identifying myocardial ischemia (AUC =0.631; P=0.058). Qian *et al.* (35) also confirmed that CCTA-based radiomic analysis of plaques was superior to conventional plaques assessment in identifying hemodynamically significant coronary stenosis.

The above studies suggest that radiomics for coronary plaques greatly increases the amount of information obtained from CCTA images, which may reveal the underlying pathophysiological processes of coronary atherosclerosis. Quantitative radiomics analysis has unique advantages over conventional methods in improving the diagnostic performance of CCTA. However, the ability of quantitative radiomics to predict MACE is still controversial as it is influenced by multiple factors and requires a larger dataset for validation (19).

Radiomics phenotyping of perivascular adipose tissue

Vascular inflammation is recognized as the key factor in the development of atherogenesis, which is the formation and rupture of vulnerable plaques that subsequently cause acute coronary syndrome (ACS) (45,46). Several studies have found that vascular inflammation shifts lipid content of PVAT in a paracrine manner via inflammatory cytokines released from the inflamed vascular wall (47-50). Antonopoulos *et al.* (47) proposed a novel imaging biomarker, the perivascular fat attenuation index (FAI), that could identify early coronary inflammation by tracking CT attenuation changes of PVAT. Recent advances have confirmed that perivascular FAI could indicate dynamic changes in local inflammatory status after ACS events and track the effects of anti-inflammatory interventions for coronary diseases (47,51,52), which has potential clinical value in cardiac risk prediction and stratification (53). However, perivascular FAI relies solely on CT attenuation to identify changes in PVAT composition without considering complex spatial information among voxels, which might lead to overlaps between pathologies. These studies highlighted that radiomics can provide quantitative spatial and textural properties to evaluate the heterogeneity

of PVAT, which may reveal underlying pathologic processes related to clinical outcomes (8).

Detection of PVAT phenotypic changes

The changes in PVAT composition are not only related to coronary inflammation, but also dysfunctional adipose tissue remodeling characterized by fibrosis and vascularity (54,55). Oikonomou *et al.* (23) primarily applied a radiotranscriptomic approach to explore the correlation between radiomics features and the biology of PVAT. By measuring relative gene expression in adipose tissue biopsies from 167 patients undergoing cardiac surgery, they detected that wavelet-transformed mean attenuation was associated with adipose tissue inflammation (*TNFA* expression) and that radiomic texture features were related to adipose tissue fibrosis (*COL1A1* expression) and vascularity (*CD31* expression). Therefore, radiomic phenotyping of PVAT was shown to capture biological characteristics of dysfunctional adipose tissue that are closely related to chronic vascular inflammation and atherosclerosis through a comprehensive analysis of attenuation, texture, and volumetric parameters.

Identification of acute myocardial infarction

Recently, a prospective case-control study Lin *et al.* (24) evaluated the ability of CCTA-based radiomic analysis of PCAT (PCAT refers to all the voxels between −190 and −30 HU range located within a radial distance from the outer vessel wall equal to the average diameter of the target vessel) to identify patients with acute myocardial infarction (MI). The study revealed that PCAT radiomic phenotypes were significantly different between patients with acute MI and those with stable or no CAD, particularly for textural and geometric radiomic features that provided additional disease-related information. A radiomic-based machine learning model was shown to have superior diagnostic performance in distinguishing patients with acute MI (AUC =0.87) compared with the PCAT attenuation-based model (AUC =0.77; P=0.001) and the clinical model (AUC =0.76; P<0.001). These findings showed that PCAT CT attenuation could only indicate a fraction of the available information by evaluating average density, which led to a rather crude variable that had an overlap of diseased patients and healthy controls. On the contrary, radiomics offered more spatial information about PCAT at a deeper level, and produced more specific radiomics phenotype that may further reveal pathophysiological changes of PCAT, which improved the ability of imaging to recognize vulnerable patients.

Improvement of cardiac risk prediction and prognosis

To evaluate the ability of PVAT radiomic phenotyping to identify patients with increased risk for MACE, Oikonomou *et al.* (23) applied a radiomics-based machine learning approach that developed a radiomic signature (fat radiomic profile; FRP) (*Figure 4*). The signature discriminated MACE from non-MACE cases within 5 years of CCTA. They also validated that FRP significantly improved MACE risk prediction in patients with CAD beyond the current state-of-the-art. In further analysis, they found that FRP did not predict non-cardiac mortality but was an independent predictor of a composite endpoint of MACE or late revascularization that confirmed the cardiac specific nature of the biomarker. This showed that FRP could provide incremental prognostic information beyond traditional risk stratification tools. More recently, in a retrospective case-control study, Shang *et al.* (28) developed and validated a radiomics-based integrated score that significantly outperformed the plaque score to identify future ACS within 3 years (AUC =0.826 *vs.* 0.640; P=0.009). This further shows the important role of radiomics information in PCAT surrounding plaques for the prediction of ACS.

Monitoring progression of post-acute MI

In a study that tested the FRP's ability to track perivascular changes over 6 months post-acute MI, Oikonomou *et al.* (23) found that FRP showed no significant changes in patients who underwent CCTA within 96 hours of acute MI and 6 months later, while FAI changed during 6 months of optimal medical therapy (23). These findings imply that FAI can capture the reversible and dynamic changes in PVAT composition in response to coronary inflammation, whereas FRP can detect more irreversible changes (such as fibrosis and vascularity) that are conducive to risk stratification. The above findings also suggest that FRP may become a powerful imaging biomarker to screen individuals undergoing CCTA for the first time. On the basis of Oikonomou *et al.*'s research (23), Lin *et al.* (24) extended to a larger population at per-patient and per-lesion level. They also found that there were no significant changes in radiomics phenotypes of PCAT in response to standard treatment within 6 months post-MI, which may further indicate that irreversible morphological changes in PCAT composition respond to coronary inflammation (54).

From the above results, it has been recognized that PVAT-based radiomics has the potential to enhance the ability to detect PVAT changes, identify vulnerable patients, improve cardiovascular risk prediction for future MACE,

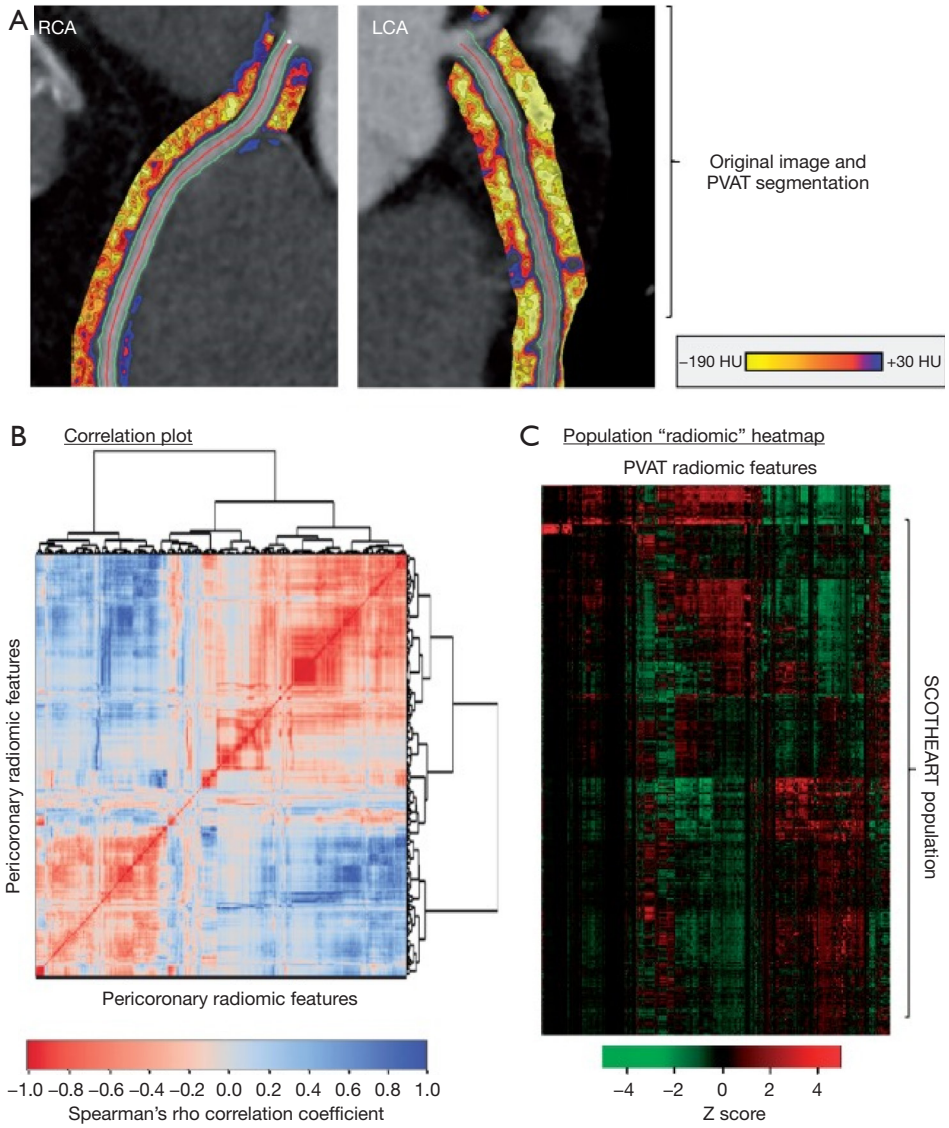

Figure 4 Radiomic phenotyping of coronary perivascular adipose tissue. The perivascular adipose tissue of the right and left coronary arteries (left main and proximal of left anterior descending artery) is used to segment and calculate radiomic statistics (A). A correlation plot with hierarchical clustering of 1,391 stable radiomic features in 1575 SCOT-HEART patients, revealing distinct clusters of radiomic variance (B). Heat map of scaled radiomic features in the SCOT-HEART population revealing between-patient variance across the cohort (C) [reproduced with permission from reference (23)]. LCA, left coronary artery; PVAT, perivascular adipose tissue; RCA, right coronary artery; SCOT-HEART, the Scottish computed tomography of the heart.

and provide additional risk stratification. Nonetheless, future testing in independent cohorts from multiple centers is still needed to refine and calibrate the radiomic models.

Radiomics phenotyping of myocardial tissue

Uneven myocardial density indicates that the arrangement of myofibrils in the myocardial tissue is irregular, which may reflect underlying myocardial pathological changes. However, non-contrast-enhanced cardiac CT is not usually applied to the diagnosis of cardiac abnormalities, except for calcium scoring of coronary arteries, because of the restrictions of intravenous contrast media and low radiation dose (56,57). Several studies have shown that texture

analysis of the left ventricle on non-contrast-enhanced cardiac CT can differentiate acute MI from healthy areas and detect high-risk phenotypes of future ACS or heart failure in participants with left ventricular hypertrophy (22,29,30). This method could further provide a clinical tool for cardiovascular risk screening. In addition, myocardial texture phenotypes on delayed iodine enhanced cardiac CT can distinguish scared tissue from normal myocardium in patients with myocarditis and detect left ventricle dilatation and systolic or diastolic function in patients with recurrent ventricular tachycardia (31,32). Furthermore, given that CCTA cannot identify and locate the target blood vessels and so cannot show a correlation between coronary stenosis and blood flow changes in the myocardium, it is of great importance to combine CCTA with other functional tests to assess chronic myocardial ischemia (MIS) comprehensively (58). Shu *et al.* (33) developed a CCTA-based radiomics nomogram that extracted radiomics features from myocardial tissue and validated the model's underlying advantages of objective and quantitative evaluation in the identification of MIS, which may assist clinicians' decision making on the diagnosis and treatment of MIS patients. All these studies show that the current application of radiomic analysis in left ventricle and myocardial tissue can identify myocardial abnormalities including ischemia, infarction, and scar formation. Despite these interesting results, they are only a few preliminary explorations, and the proposed radiomic phenotypes need to be further validated in independent cohorts.

Radiomics phenotyping of intracardiac lesions

It is essential to accurately differentiate the etiologies behind intracardiac lesions with a non-invasive method because different etiologies require different treatment strategies. However, the current assessment methods remain limited by the low specificity of clinical and imaging manifestations of intracardiac lesions. Nam *et al.* (34), in a single-center retrospective study of differentiation of the etiologies behind prosthetic valve obstruction, found that the radiomic score of the periprosthetic mass outperformed visual analysis when differentiating pannus from other abnormalities in patients with suspected prosthetic valve obstruction. Qian *et al.* (35) developed a radiomics signature based on contrast-enhanced CT images and verified that it performed better than the conventional clinical model at differentiating cardiac myxomas from thrombi. Moreover, Chun *et al.* (36) showed that radiomic features from single-phase cardiac CT performed better when discriminating left atrial appendage thrombus from circulatory stasis in patients with valvular heart disease than left atrial appendage/ascending aorta values. These studies imply that radiomics could establish a link between imaging phenotyping and etiology of lesions in patients with valvular heart disease, improve diagnostic accuracy for the presence of filling defect or periprosthetic mass, and contribute to guiding effective treatment strategy.

Overall, the current applications of cardiac CT radiomics in cardiovascular disease highlight its value in identifying vulnerable plaques or vulnerable patients, improving cardiac risk prediction and stratification, and discriminating myocardial pathology and etiologies behind intracardiac lesions. Recent research progress in coronary PVAT radiomics has further expanded the potential of cardiac CT radiomics and offered a new perspective for further development of personalized cardiovascular medicine.

Radiomics challenges

The process of radiomics has limitations that impact its implementation in clinical practice. Although the Quantitative Imaging Biomarkers Alliance founded by Radiological Society of North America and the European Imaging Biomarkers Alliance established by European Society of Radiology proposed to facilitate the development of radiomics and improve the performance of quantitative parameters, current radiomic technologies still need to overcome the technical complexity that affects their daily clinical applications (8). The standardization of acquisition protocols and data analysis techniques needs to be further established to offer a robust framework for radiomic analysis (24). Furthermore, the reproducibility of radiomic features is affected by a series of factors including image acquisition, reconstruction, and analysis (59-61). The generalizability of developed radiomics models may also be limited due to radiomic metrics from the same CT scanner and protocol in a single center. Therefore, large clinical trials with different protocols from multi-center studies are still essential to verify the results derived from radiomic analysis (26).

There are some urgent problems related to cardiac CT imaging limited the development of cardiovascular radiomics. First, oncology research can easily obtain pathological results, but cardiovascular research is usually based on invasive FFR or follow-up results as the gold standard, which limits the development of cardiovascular

radiomics to a certain extent. Second, tumor segmentation can be performed by delineating the ROI along the edge of the tumor, yet the boundaries of some lesions in cardiac CT images are relatively blurred. Manual segmentation may cause higher interobserver variability and lower efficiency because the success of the procedure depends on the expertise of radiologists. Although fully automatic segmentation can reduce the heterogeneity of lesions and improve efficiency to some extent, it still cannot guarantee accuracy of interpretation (62). Moreover, regarding the segmentation process of cardiac CT images, some limitations remain because the process has not been standardized yet. Establishing a widely recognized and accepted segmentation method aimed at cardiac CT images will help to address the current challenges.

Future directions

Although radiomic phenotyping has the potential to identify the anatomic and metabolic characteristics of vulnerable plaques, the current research is still a long way from guiding clinical decision-making. Recently, some scholars committed to developing automatic segmentation software for coronary plaques, which are expected to detect more novel imaging biomarkers that are closely associated with future MACE in CAD patients. Furthermore, with the advancements of computational techniques, further studies are needed to explore the differences of radiomic phenotyping between culprit and non-culprit plaques to detect vulnerable patients. Moreover, Eslami *et al.* (63) extracted radiomic features from coronary artery calcium (CAC) based on non-contrast cardiac CT. They developed a radiomic-based score including the complex properties of CAC and showed that it improved the ability to identify individuals at risk for MACE. Future studies may further explore its potential value to evaluate drug effects, guide revascularization, and improve prognosis (62).

Developing automatic segmentation software will further provide more possibilities for PCAT radiomics to explore more novel biomarkers for diagnostic, prognostic, and therapeutical decisions. Given the variable anatomy and small caliber of the left circumflex coronary artery, as described previously in the CRISP-CT study (53), current studies have mainly extracted radiomics features from PVAT surrounding the left anterior descending artery and right coronary artery (23). Subsequent research could introduce PVAT radiomics surrounding the left circumflex artery to evaluate its value for cardiac risk prediction and stratification. Additionally, radiomics analysis on PCAT at the per-patient and per-lesion level can capture the persistent structural remodeling of PCAT in patients with acute MI and 6 months after MI (23,24). Future directions can assess whether PCAT radiomics could provide significant prognostic information for recurrent MACE in patients with acute MI after revascularization. Some studies have shown that epicardial fat dysfunction may be linked to early plaque formation and inflammation (64). Therefore, epicardial fat radiomics based on cardiac CT is likely to be a future hotspot in the cardiovascular field.

Cardiac magnetic resonance (CMR) radiomics has prominent advantages over conventional cardiac CT when identifying myocardial abnormalities (65). However, the application of radiomics for delayed enhancement cardiac CT may provide more information about myocardial characterization and promote the transition of imaging methods from CMR to cardiac CT to a certain degree. Therefore, future research should expand on this and further probe the value of cardiac CT radiomics in the myocardium. To date, CT perfusion radiomics has not been deeply explored in the cardiovascular field, but this is urgently required. Finally, the current research trend of radiomics is beginning to combine with deep learning. Using the extracted radiomics features to build a deep learning network or extracting deep learning features and substituting them into the machine learning model of radiomics will be the hotspots and trends of future development.

Study strengths and limitations

This narrative review provides an update on the current applications of cardiac CT radiomics, which contributes to future research in the diagnosis and prognosis of cardiovascular diseases. Nonetheless, there were still some limitations to this narrative review: It is illustrative instead of exhaustive. Some of the opinions in this review may also be subjective to interpretations based on our own clinical and research experience about cardiovascular radiomics and should be considered as references rather than clinical recommendations. Furthermore, the findings are subject to change in line with the rapid development of radiomics technology and clinical applications.

Conclusions

Cardiac CT radiomics can detect disease-related additional

information at a microstructural level and establish a link between imaging phenotyping and tissue pathology or biology. This has significant clinical implications and can contribute to clinical decision-making. However, cardiac CT radiomics is still in its infancy and has many challenges to overcome before it can be applied to clinical practice. With advancements of cardiac CT imaging, the standardization of the radiomics process, and the development of automatic segmentation software, cardiac CT radiomics is expected to provide more precise phenotyping of cardiovascular disease for patients and doctors, which will improve diagnostic, prognostic, and therapeutical decisions in the future.

Acknowledgments

Funding: This work was supported by the National Natural Science Foundation (Nos. 82071920 and 81901741), the Key Research & Development Plan of Liaoning Province (No. 2020JH2/10300037), and 345 Talent Project in Shengjing Hospital of China Medical University and Outstanding Scientific Fund of Shengjing Hospital.

Footnote

Reporting Checklist: The authors have completed the Narrative Review reporting checklist. Available at https://qims.amegroups.com/article/view/10.21037/qims-21-1022/rc

Conflicts of Interest: All authors have completed the ICMJE uniform disclosure form (available at https://qims.amegroups.com/article/view/10.21037/qims-21-1022/coif). YG is an employee of GE Healthcare. The other authors have no conflicts of interest to declare.

Ethical Statement: The authors are accountable for all aspects of the work in ensuring that questions related to the accuracy or integrity of any part of the work are appropriately investigated and resolved.

References

1. Williams MC, Hunter A, Shah ASV, Assi V, Lewis S, Smith J, Berry C, Boon NA, Clark E, Flather M, Forbes J, McLean S, Roditi G, van Beek EJR, Timmis AD, Newby DE; SCOT-HEART Investigators. Use of Coronary Computed Tomographic Angiography to Guide Management of Patients With Coronary Disease. J Am Coll Cardiol 2016;67:1759-68.
2. Cheruvu C, Precious B, Naoum C, Blanke P, Ahmadi A, Soon J, et al. Long term prognostic utility of coronary CT angiography in patients with no modifiable coronary artery disease risk factors: Results from the 5 year follow-up of the CONFIRM International Multicenter Registry. J Cardiovasc Comput Tomogr 2016;10:22-7.
3. Budoff MJ, Dowe D, Jollis JG, Gitter M, Sutherland J, Halamert E, Scherer M, Bellinger R, Martin A, Benton R, Delago A, Min JK. Diagnostic performance of 64-multidetector row coronary computed tomographic angiography for evaluation of coronary artery stenosis in individuals without known coronary artery disease: results from the prospective multicenter ACCURACY (Assessment by Coronary Computed Tomographic Angiography of Individuals Undergoing Invasive Coronary Angiography) trial. J Am Coll Cardiol 2008;52:1724-32.
4. Shaw LJ, Min JK, Hachamovitch R, Peterson ED, Hendel RC, Woodard PK, Berman DS, Douglas PS. Cardiovascular imaging research at the crossroads. JACC Cardiovasc Imaging 2010;3:316-24.
5. Douglas PS, Hoffmann U, Patel MR, Mark DB, Al-Khalidi HR, Cavanaugh B, et al. Outcomes of anatomical versus functional testing for coronary artery disease. N Engl J Med 2015;372:1291-300.
6. Nicol ED, Norgaard BL, Blanke P, Ahmadi A, Weir-McCall J, Horvat PM, Han K, Bax JJ, Leipsic J. The Future of Cardiovascular Computed Tomography: Advanced Analytics and Clinical Insights. JACC Cardiovasc Imaging 2019;12:1058-72.
7. Task Force Members, Montalescot G, Sechtem U, Achenbach S, Andreotti F, Arden C, et al. 2013 ESC guidelines on the management of stable coronary artery disease: the Task Force on the management of stable coronary artery disease of the European Society of Cardiology. Eur Heart J 2013;34:2949-3003.
8. Kolossváry M, Kellermayer M, Merkely B, Maurovich-Horvat P. Cardiac Computed Tomography Radiomics:

A Comprehensive Review on Radiomic Techniques. J Thorac Imaging 2018;33:26-34.
9. Barabási AL, Gulbahce N, Loscalzo J. Network medicine: a network-based approach to human disease. Nat Rev Genet 2011;12:56-68.
10. Bickelhaupt S, Paech D, Kickingereder P, Steudle F, Lederer W, Daniel H, Götz M, Gählert N, Tichy D, Wiesenfarth M, Laun FB, Maier-Hein KH, Schlemmer HP, Bonekamp D. Prediction of malignancy by a radiomic signature from contrast agent-free diffusion MRI in suspicious breast lesions found on screening mammography. J Magn Reson Imaging 2017;46:604-16.
11. Huang Y, Liu Z, He L, Chen X, Pan D, Ma Z, Liang C, Tian J, Liang C. Radiomics Signature: A Potential Biomarker for the Prediction of Disease-Free Survival in Early-Stage (I or II) Non-Small Cell Lung Cancer. Radiology 2016;281:947-57.
12. Prasanna P, Patel J, Partovi S, Madabhushi A, Tiwari P. Radiomic features from the peritumoral brain parenchyma on treatment-naïve multi-parametric MR imaging predict long versus short-term survival in glioblastoma multiforme: Preliminary findings. Eur Radiol 2017;27:4188-97.
13. Li H, Zhu Y, Burnside ES, Drukker K, Hoadley KA, Fan C, Conzen SD, Whitman GJ, Sutton EJ, Net JM, Ganott M, Huang E, Morris EA, Perou CM, Ji Y, Giger ML. MR Imaging Radiomics Signatures for Predicting the Risk of Breast Cancer Recurrence as Given by Research Versions of MammaPrint, Oncotype DX, and PAM50 Gene Assays. Radiology 2016;281:382-91.
14. Kickingereder P, Götz M, Muschelli J, Wick A, Neuberger U, Shinohara RT, Sill M, Nowosielski M, Schlemmer HP, Radbruch A, Wick W, Bendszus M, Maier-Hein KH, Bonekamp D. Large-scale Radiomic Profiling of Recurrent Glioblastoma Identifies an Imaging Predictor for Stratifying Anti-Angiogenic Treatment Response. Clin Cancer Res 2016;22:5765-71.
15. Coroller TP, Agrawal V, Huynh E, Narayan V, Lee SW, Mak RH, Aerts HJWL. Radiomic-Based Pathological Response Prediction from Primary Tumors and Lymph Nodes in NSCLC. J Thorac Oncol 2017;12:467-76.
16. Lambin P, Leijenaar RTH, Deist TM, Peerlings J, de Jong EEC, van Timmeren J, Sanduleanu S, Larue RTHM, Even AJG, Jochems A, van Wijk Y, Woodruff H, van Soest J, Lustberg T, Roelofs E, van Elmpt W, Dekker A, Mottaghy FM, Wildberger JE, Walsh S. Radiomics: the bridge between medical imaging and personalized medicine. Nat Rev Clin Oncol 2017;14:749-62.
17. Zwanenburg A, Leger S, Vallieres M, Lock S. Image biomarker standardisation initiative. arXiv preprint 2016;arXiv:1612.07003.
18. Kolossváry M, Karády J, Szilveszter B, Kitslaar P, Hoffmann U, Merkely B, Maurovich-Horvat P. Radiomic Features Are Superior to Conventional Quantitative Computed Tomographic Metrics to Identify Coronary Plaques With Napkin-Ring Sign. Circ Cardiovasc Imaging 2017;10:e006843.
19. Hu W, Wu X, Dong D, Cui LB, Jiang M, Zhang J, Wang Y, Wang X, Gao L, Tian J, Cao F. Novel radiomics features from CCTA images for the functional evaluation of significant ischaemic lesions based on the coronary fractional flow reserve score. Int J Cardiovasc Imaging 2020;36:2039-50.
20. Kolossváry M, Karády J, Kikuchi Y, Ivanov A, Schlett CL, Lu MT, Foldyna B, Merkely B, Aerts HJ, Hoffmann U, Maurovich-Horvat P. Radiomics versus Visual and Histogram-based Assessment to Identify Atheromatous Lesions at Coronary CT Angiography: An ex Vivo Study. Radiology 2019;293:89-96.
21. Kolossváry M, Park J, Bang JI, Zhang J, Lee JM, Paeng JC, Merkely B, Narula J, Kubo T, Akasaka T, Koo BK, Maurovich-Horvat P. Identification of invasive and radionuclide imaging markers of coronary plaque vulnerability using radiomic analysis of coronary computed tomography angiography. Eur Heart J Cardiovasc Imaging 2019;20:1250-8.
22. Hinzpeter R, Wagner MW, Wurnig MC, Seifert B, Manka R, Alkadhi H. Texture analysis of acute myocardial infarction with CT: First experience study. PLoS One 2017;12:e0186876.
23. Oikonomou EK, Williams MC, Kotanidis CP, Desai MY, Marwan M, Antonopoulos AS, et al. A novel machine learning-derived radiotranscriptomic signature of perivascular fat improves cardiac risk prediction using coronary CT angiography. Eur Heart J 2019;40:3529-43.
24. Lin A, Kolossváry M, Yuvaraj J, Cadet S, McElhinney PA, Jiang C, Nerlekar N, Nicholls SJ, Slomka PJ, Maurovich-Horvat P, Wong DTL, Dey D. Myocardial Infarction Associates With a Distinct Pericoronary Adipose Tissue Radiomic Phenotype: A Prospective Case-Control Study. JACC Cardiovasc Imaging 2020;13:2371-83.
25. Oikonomou EK, Siddique M, Antoniades C. Artificial intelligence in medical imaging: A radiomic guide to precision phenotyping of cardiovascular disease. Cardiovasc Res 2020;116:2040-54.
26. Gillies RJ, Kinahan PE, Hricak H. Radiomics: Images

Are More than Pictures, They Are Data. Radiology 2016;278:563-77.
27. Li L, Hu X, Tao X, Shi X, Zhou W, Hu H, Hu X. Radiomic features of plaques derived from coronary CT angiography to identify hemodynamically significant coronary stenosis, using invasive FFR as the reference standard. Eur J Radiol 2021;140:109769.
28. Shang J, Ma S, Guo Y, Yang L, Zhang Q, Xie F, Ma Y, Ma Q, Dang Y, Zhou K, Liu T, Yang J, Hou Y. Prediction of acute coronary syndrome within 3 years using radiomics signature of pericoronary adipose tissue based on coronary computed tomography angiography. Eur Radiol 2022;32:1256-66.
29. Mannil M, von Spiczak J, Manka R, Alkadhi H. Texture Analysis and Machine Learning for Detecting Myocardial Infarction in Noncontrast Low-Dose Computed Tomography: Unveiling the Invisible. Invest Radiol 2018;53:338-43.
30. Kay FU, Abbara S, Joshi PH, Garg S, Khera A, Peshock RM. Identification of High-Risk Left Ventricular Hypertrophy on Calcium Scoring Cardiac Computed Tomography Scans: Validation in the DHS. Circ Cardiovasc Imaging 2020;13:e009678.
31. Antunes S, Esposito A, Palmisanov A, Colantoni C, de Cobelli F, Del Maschio A. Characterization of normal and scarred myocardium based on texture analysis of cardiac computed tomography images. Annu Int Conf IEEE Eng Med Biol Soc 2016;2016:4161-4.
32. Esposito A, Palmisano A, Antunes S, Colantoni C, Rancoita PMV, Vignale D, Baratto F, Della Bella P, Del Maschio A, De Cobelli F. Assessment of Remote Myocardium Heterogeneity in Patients with Ventricular Tachycardia Using Texture Analysis of Late Iodine Enhancement (LIE) Cardiac Computed Tomography (cCT) Images. Mol Imaging Biol 2018;20:816-25.
33. Shu ZY, Cui SJ, Zhang YQ, Xu YY, Hung SC, Fu LP, Pang PP, Gong XY, Jin QY. Predicting Chronic Myocardial Ischemia Using CCTA-Based Radiomics Machine Learning Nomogram. J Nucl Cardiol 2022;29:262-74.
34. Nam K, Suh YJ, Han K, Park SJ, Kim YJ, Choi BW. Value of Computed Tomography Radiomic Features for Differentiation of Periprosthetic Mass in Patients With Suspected Prosthetic Valve Obstruction. Circ Cardiovasc Imaging 2019;12:e009496.
35. Qian WL, Jiang Y, Liu X, Guo YK, Li Y, Tang X, Yang ZG. Distinguishing cardiac myxomas from cardiac thrombi by a radiomics signature based on cardiovascular contrast-enhanced computed tomography images. BMC Cardiovasc Disord 2021;21:152.
36. Chun SH, Suh YJ, Han K, Park SJ, Shim CY, Hong GR, Lee S, Lee SH, Kim YJ, Choi BW. Differentiation of left atrial appendage thrombus from circulatory stasis using cardiac CT radiomics in patients with valvular heart disease. Eur Radiol 2021;31:1130-9.
37. Williams MC, Moss AJ, Dweck M, Adamson PD, Alam S, Hunter A, Shah ASV, Pawade T, Weir-McCall JR, Roditi G, van Beek EJR, Newby DE, Nicol ED. Coronary Artery Plaque Characteristics Associated With Adverse Outcomes in the SCOT-HEART Study. J Am Coll Cardiol 2019;73:291-301.
38. Motoyama S, Ito H, Sarai M, Kondo T, Kawai H, Nagahara Y, Harigaya H, Kan S, Anno H, Takahashi H, Naruse H, Ishii J, Hecht H, Shaw LJ, Ozaki Y, Narula J. Plaque Characterization by Coronary Computed Tomography Angiography and the Likelihood of Acute Coronary Events in Mid-Term Follow-Up. J Am Coll Cardiol 2015;66:337-46.
39. Puchner SB, Liu T, Mayrhofer T, Truong QA, Lee H, Fleg JL, Nagurney JT, Udelson JE, Hoffmann U, Ferencik M. High-risk plaque detected on coronary CT angiography predicts acute coronary syndromes independent of significant stenosis in acute chest pain: results from the ROMICAT-II trial. J Am Coll Cardiol 2014;64:684-92.
40. Lee JM, Choi G, Koo BK, Hwang D, Park J, Zhang J, et al. Identification of High-Risk Plaques Destined to Cause Acute Coronary Syndrome Using Coronary Computed Tomographic Angiography and Computational Fluid Dynamics. JACC Cardiovasc Imaging 2019;12:1032-43.
41. Otsuka K, Fukuda S, Tanaka A, Nakanishi K, Taguchi H, Yoshikawa J, Shimada K, Yoshiyama M. Napkin-ring sign on coronary CT angiography for the prediction of acute coronary syndrome. JACC Cardiovasc Imaging 2013;6:448-57.
42. Ferencik M, Hoffmann U. High-Risk Coronary Plaque on Computed Tomography Angiography: Time to Recognize a New Imaging Risk Factor. Circ Cardiovasc Imaging 2018;11:e007288.
43. Lee JM, Choi KH, Koo BK, Park J, Kim J, Hwang D, et al. Prognostic Implications of Plaque Characteristics and Stenosis Severity in Patients With Coronary Artery Disease. J Am Coll Cardiol 2019;73:2413-24.
44. Oikonomou EK, West HW, Antoniades C. Cardiac Computed Tomography: Assessment of Coronary Inflammation and Other Plaque Features. Arterioscler Thromb Vasc Biol 2019;39:2207-19.
45. Ross R. Atherosclerosis--an inflammatory disease. N Engl

J Med 1999;340:115-26.
46. Momiyama Y, Adachi H, Fairweather D, Ishizaka N, Saita E. Inflammation, Atherosclerosis and Coronary Artery Disease. Clin Med Insights Cardiol 2016;8:67-70.
47. Antonopoulos AS, Sanna F, Sabharwal N, Thomas S, Oikonomou EK, Herdman L, et al. Detecting human coronary inflammation by imaging perivascular fat. Sci Transl Med 2017;9:eaal2658.
48. Margaritis M, Antonopoulos AS, Digby J, Lee R, Reilly S, Coutinho P, Shirodaria C, Sayeed R, Petrou M, De Silva R, Jalilzadeh S, Demosthenous M, Bakogiannis C, Tousoulis D, Stefanadis C, Choudhury RP, Casadei B, Channon KM, Antoniades C. Interactions between vascular wall and perivascular adipose tissue reveal novel roles for adiponectin in the regulation of endothelial nitric oxide synthase function in human vessels. Circulation 2013;127:2209-21.
49. Antonopoulos AS, Margaritis M, Coutinho P, Shirodaria C, Psarros C, Herdman L, Sanna F, De Silva R, Petrou M, Sayeed R, Krasopoulos G, Lee R, Digby J, Reilly S, Bakogiannis C, Tousoulis D, Kessler B, Casadei B, Channon KM, Antoniades C. Adiponectin as a link between type 2 diabetes and vascular NADPH oxidase activity in the human arterial wall: the regulatory role of perivascular adipose tissue. Diabetes 2015;64:2207-19.
50. Grant RW, Stephens JM. Fat in flames: influence of cytokines and pattern recognition receptors on adipocyte lipolysis. Am J Physiol Endocrinol Metab 2015;309:E205-13.
51. Goeller M, Achenbach S, Cadet S, Kwan AC, Commandeur F, Slomka PJ, Gransar H, Albrecht MH, Tamarappoo BK, Berman DS, Marwan M, Dey D. Pericoronary Adipose Tissue Computed Tomography Attenuation and High-Risk Plaque Characteristics in Acute Coronary Syndrome Compared With Stable Coronary Artery Disease. JAMA Cardiol 2018;3:858-63.
52. Kwiecinski J, Dey D, Cadet S, Lee SE, Otaki Y, Huynh PT, Doris MK, Eisenberg E, Yun M, Jansen MA, Williams MC, Tamarappoo BK, Friedman JD, Dweck MR, Newby DE, Chang HJ, Slomka PJ, Berman DS. Peri-Coronary Adipose Tissue Density Is Associated With 18F-Sodium Fluoride Coronary Uptake in Stable Patients With High-Risk Plaques. JACC Cardiovasc Imaging 2019;12:2000-10.
53. Oikonomou EK, Marwan M, Desai MY, Mancio J, Alashi A, Hutt Centeno E, et al. Non-invasive detection of coronary inflammation using computed tomography and prediction of residual cardiovascular risk (the CRISP CT study): a post-hoc analysis of prospective outcome data. Lancet 2018;392:929-39.
54. Crewe C, An YA, Scherer PE. The ominous triad of adipose tissue dysfunction: inflammation, fibrosis, and impaired angiogenesis. J Clin Invest 2017;127:74-82.
55. Oikonomou EK, Antoniades C. The role of adipose tissue in cardiovascular health and disease. Nat Rev Cardiol 2019;16:83-99.
56. Liew G, Chow C, van Pelt N, Younger J, Jelinek M, Chan J, Hamilton-Craig C. Cardiac Society of Australia and New Zealand Position Statement: Coronary Artery Calcium Scoring. Heart Lung Circ 2017;26:1239-51.
57. Baron KB, Choi AD, Chen MY. Low Radiation Dose Calcium Scoring: Evidence and Techniques. Curr Cardiovasc Imaging Rep 2016;9:12.
58. Ozaki Y, Okumura M, Ismail TF, Motoyama S, Naruse H, Hattori K, Kawai H, Sarai M, Takagi Y, Ishii J, Anno H, Virmani R, Serruys PW, Narula J. Coronary CT angiographic characteristics of culprit lesions in acute coronary syndromes not related to plaque rupture as defined by optical coherence tomography and angioscopy. Eur Heart J 2011;32:2814-23.
59. Berenguer R, Pastor-Juan MDR, Canales-Vázquez J, Castro-García M, Villas MV, Mansilla Legorburo F, Sabater S. Radiomics of CT Features May Be Nonreproducible and Redundant: Influence of CT Acquisition Parameters. Radiology 2018;288:407-15.
60. Shafiq-Ul-Hassan M, Zhang GG, Latifi K, Ullah G, Hunt DC, Balagurunathan Y, Abdalah MA, Schabath MB, Goldgof DG, Mackin D, Court LE, Gillies RJ, Moros EG. Intrinsic dependencies of CT radiomic features on voxel size and number of gray levels. Med Phys 2017;44:1050-62.
61. Kolossváry M, Szilveszter B, Karády J, Drobni ZD, Merkely B, Maurovich-Horvat P. Effect of image reconstruction algorithms on volumetric and radiomic parameters of coronary plaques. J Cardiovasc Comput Tomogr 2019;13:325-30.
62. Xu P, Xue Y, Schoepf UJ, Varga-Szemes A, Griffith J, Yacoub B, Zhou F, Zhou C, Yang Y, Xing W, Zhang L. Radiomics: The Next Frontier of Cardiac Computed Tomography. Circ Cardiovasc Imaging 2021;14:e011747.
63. Eslami P, Parmar C, Foldyna B, Scholtz JE, Ivanov A, Zeleznik R, Lu MT, Ferencik M, Vasan RS, Baltrusaitis K, Massaro JM, D'Agostino RB, Mayrhofer T, O'Donnell CJ, Aerts HJWL, Hoffmann U. Radiomics of Coronary Artery Calcium in the Framingham Heart Study. Radiol Cardiothorac Imaging 2020;2:e190119.

64. Mancio J, Azevedo D, Saraiva F, Azevedo AI, Pires-Morais G, Leite-Moreira A, Falcao-Pires I, Lunet N, Bettencourt N. Epicardial adipose tissue volume assessed by computed tomography and coronary artery disease: a systematic review and meta-analysis. Eur Heart J Cardiovasc Imaging 2018;19:490-7.

65. Raisi-Estabragh Z, Izquierdo C, Campello VM, Martin-Isla C, Jaggi A, Harvey NC, Lekadir K, Petersen SE. Cardiac magnetic resonance radiomics: basic principles and clinical perspectives. Eur Heart J Cardiovasc Imaging 2020;21:349-56.

Cite this article as: Shang J, Guo Y, Ma Y, Hou Y. Cardiac computed tomography radiomics: a narrative review of current status and future directions. Quant Imaging Med Surg 2022;12(6):3436-3453. doi: 10.21037/qims-21-1022

